Design of a tuned mass damper for high quality factor suspension modes in Advanced LIGO

N. A. Robertson, P. Fritschel, B. Shapiro, C. I. Torrie, and M. Evans

Citation: Review of Scientific Instruments **88**, 035117 (2017); doi: 10.1063/1.4978796
View online: http://dx.doi.org/10.1063/1.4978796
View Table of Contents: http://aip.scitation.org/toc/rsi/88/3
Published by the American Institute of Physics

REVIEW OF SCIENTIFIC INSTRUMENTS **88**, 035117 (2017)

Design of a tuned mass damper for high quality factor suspension modes in Advanced LIGO

N. A. Robertson,[1,a),b)] P. Fritschel,[2] B. Shapiro,[3] C. I. Torrie,[1] and M. Evans[2]
[1]*LIGO, California Institute of Technology, Pasadena, California 91125, USA*
[2]*LIGO, Massachusetts Institute of Technology, Cambridge, Massachusetts 02139, USA*
[3]*Stanford University, Stanford, California 94305, USA*

(Received 10 January 2017; accepted 4 March 2017; published online 30 March 2017)

We discuss the requirements, design, and performance of a tuned mass damper which we have developed to damp the highest frequency pendulum modes of the quadruple suspensions which support the test masses in the two advanced detectors of the Laser Interferometric Gravitational-Wave Observatory. The design has to meet the requirements on mass, size, and level of damping to avoid unduly compromising the suspension thermal noise performance and to allow retrofitting of the dampers to the suspensions with minimal changes to the existing suspensions. We have produced a design satisfying our requirements which can reduce the quality factor of these modes from ~500 000 to less than 10 000, reducing the time taken for the modes to damp down from several hours to a few minutes or less. *Published by AIP Publishing.* [http://dx.doi.org/10.1063/1.4978796]

I. INTRODUCTION

2016 has been a landmark year for physics and astronomy with the announcement of the first direct detection of gravitational waves by LIGO, the Laser Interferometric Gravitational-Wave Observatory, from the inspiral and coalescence of two stellar mass black holes.[1] With a second detection announced a few months later, we are seeing the dawn of a new field of astronomy.[2] These first detections were made by Advanced LIGO,[3] an upgrade to the original LIGO detectors with improved sensitivity and wider bandwidth of operation.[4] Detecting these waves has been extremely challenging, requiring the ability to sense strains in space of order 10^{-21} at frequencies from a few 10's of Hz to a few kHz. One of the key challenges was to design a suspension system for the test masses which would provide sufficient isolation from seismic disturbances and would minimize the displacements due to suspension thermal noise. These requirements led to the design of a quadruple pendulum incorporating three stages of maraging steel blade springs for enhanced vertical isolation. To minimize the thermal noise associated with the pendulum modes of the suspension, the final (lowest) stage consists of a silica mirror, 40 kg in mass, suspended from another silica mass by four silica fibers welded to silica ears bonded to the sides of the masses. The final stage is thus essentially a monolithic fused silica suspension, as shown in Figure 1. The design of the quadruple pendulum suspension was chosen to achieve a displacement noise level for each of the seismic noise and thermal noise contributions of 10^{-19} m/$\sqrt{\text{Hz}}$ at 10 Hz, for each test mass. For further details of the design see Aston *et al.*[5] and Cumming *et al.*[6]

The quadruple pendulum has 24 rigid body (pendulum) modes. Electronic sensing and feedback applied to the top mass is used to damp 22 of these modes which by design lie in a frequency range of ~0.4–5 Hz. The two highest frequency modes, which are the highest vertical (bounce) and roll modes at around 9.7 and 13.8 Hz, respectively, involve extension of the silica fibers between the penultimate and test masses, as indicated in Figure 1. These modes are sufficiently far away from the lower frequency modes that they are very weakly coupled to external forces and they remain undamped by the electronic feedback. The modes have very high quality factors, Q, due to the intrinsic low mechanical loss of silica, which is preserved by the monolithic design of the final stage of the quadruple suspension. Such a design ensures that the off-resonance level of suspension thermal noise at the frequencies of operation of the detector is sufficiently low to meet our noise requirements. Typical measured values of Q for these modes in vacuum are in range $(4–6) \times 10^5$.

Unfortunately such high Qs come with a price. When the interferometer experiences a large disturbance such as an earthquake, the bounce and roll modes can get excited to levels several orders of magnitude higher than normal and take a long time to decay again. The degree to which this occurred was more than we had anticipated in the design phase. It is possible to actively damp these modes, using interferometric sensor signals generated within the interferometer to apply damping forces to the penultimate masses. However, this method relies on weak and possibly variable cross coupling of these modes into other degrees-of-freedom, both for sensing and actuation. It could thus take up to several hours for active damping to suppress the modes sufficiently for sensitive interferometer operation. While active damping allowed us to operate during the first observing run of Advanced LIGO in which we made the historic first detection, it was not a robust, efficient solution.

To reduce the amount of operating time lost to controlling these modes when rung up, one could consider actively damping the modes more effectively by introducing sensors and actuators in the vertical and roll degrees of freedom at

[a)]Author to whom correspondence should be addressed. Electronic mail: nroberts@ligo.caltech.edu.
[b)]Also at SUPA, University of Glasgow, Glasgow G12 8QQ, United Kingdom.

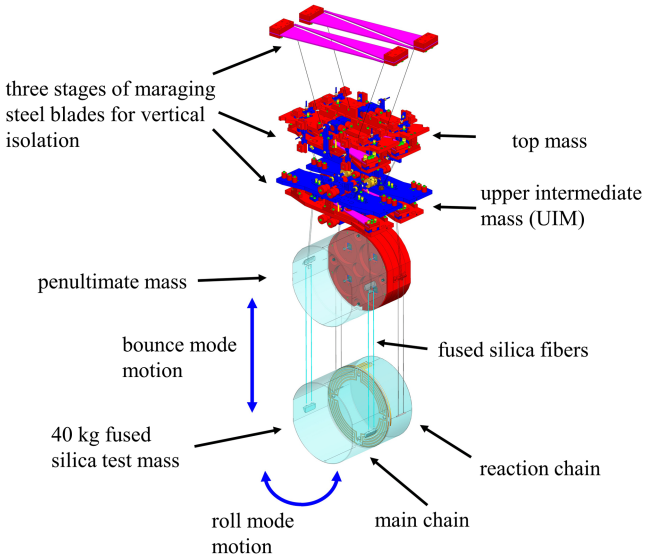

FIG. 1. Drawing of the Advanced LIGO quadruple pendulum suspension. The system consists of a main chain supporting the test mass, and a parallel reaction chain behind it, which is used for applying actuation forces. The motions involved in the two modes to be damped are indicated by the double ended arrows.

the penultimate or test mass itself. However even with the best displacement sensors such as a compact interferometric sensor[7] with noise level of $\sim 10^{-12}$ m/$\sqrt{\text{Hz}}$ at 10 Hz, sensor noise imposed by the feedback loop would spoil the intrinsic low noise performance of the suspension. Instead, we have developed passive tuned mass dampers which can be easily retrofitted to our existing suspensions and which reduce the damping time from hours to of order 100 s. We call these dampers BRDs from their application as Bounce and Roll Dampers.

Figure 2 illustrates the concept of a tuned mass damper. A one degree of freedom undamped system consists of a mass M and stiffness K. Without damping, this system is susceptible to large mechanical oscillations at its natural frequency. These oscillations can be damped by coupling to it another, relatively small, single degree of freedom system consisting of mass m and lossy spring $k(1 + i\phi)$, where $i\phi$ is the imaginary mechanical loss factor according to the structural damping

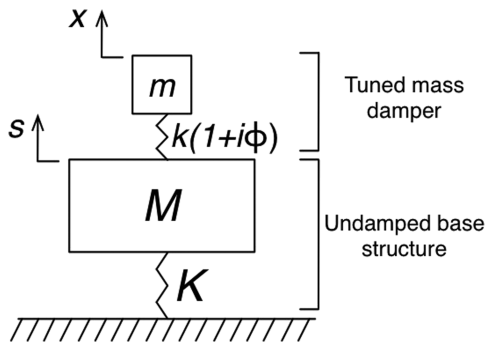

FIG. 2. Schematic sketch of a generalized tuned mass damper. The undamped base structure consists of mass M, spring stiffness K, and displacement s. The mechanical resonance of this structure is damped by the addition of the tuned mass damper consisting of mass m, lossy spring $k(1 + i\phi)$, and displacement x, where $i\phi$ is the imaginary mechanical loss factor according to the structural damping model.

model. Careful tuning of the natural frequency of the tuned mass damper results in maximized damping for a given damper mass m. Larger damper masses permit greater damping.

In Section II we present the requirements for the BRDs based on simulations of the dynamics of the quadruple pendulum with dampers attached. We discuss the general features of the BRD design in Section III. In Section IV we describe our results from testing various prototypes on a mock-up of the lower stages of a quadruple pendulum in the laboratory at Caltech, leading to a final design. In Section V we present results and conclusions from applying the dampers *in situ* in the LIGO detector at Livingston, Louisiana.

II. REQUIREMENTS AND SIMULATIONS

The use of fused silica fibers in the final stage of the quadruple pendulum was chosen to allow us to achieve a predicted displacement noise level in the longitudinal direction (the direction sensed by the laser interferometer) from thermal noise contributions at or below 10^{-19} m/$\sqrt{\text{Hz}}$ above 10 Hz, as shown in Figure 8 of Aston *et al.*[5] The addition of passive damping of the highest bounce and roll modes will raise the thermal noise level in the longitudinal direction due to the cross coupling of motion from vertical and roll into longitudinal, in particular around the two mode frequencies in the 10–14 Hz region. We wish to limit this increase so that by 20 Hz the additional thermal noise due to the BRDs has fallen to a level significantly below the intrinsic thermal noise in the longitudinal direction without the dampers. This intrinsic noise is $\sim 1.6 \times 10^{-20}$ m/$\sqrt{\text{Hz}}$.[5] Additionally, the dampers should damp the modes so that the decay time constant is about 100 s. To investigate the implications on the design from these requirements, we developed a state space model of the quadruple pendulum with tuned mass dampers attached. By applying the fluctuation-dissipation theorem, we estimate the thermal noise of the system as a function of key parameters of the BRD design. This in turn can be used to allow us to choose a set of parameters which can meet the thermal noise and the damping time requirements.

A. State space modelling and thermal noise estimation

Detailed calculations and thermal noise simulations for the BRDs are given in Shapiro.[8] This section summarizes those calculations.

The displacement noise due to thermal noise from the BRDs seen by the interferometer, N, in m/$\sqrt{\text{Hz}}$, is given by applying a model of the BRD damped suspension to the fluctuation-dissipation theorem shown in the following equation:[9]

$$N = \frac{C}{\pi f}\sqrt{K_B T\,|\Re\,(Y\,(f))|}, \tag{1}$$

where C is a coupling factor from a given degree of freedom into the longitudinal direction, f is the frequency in Hz, K_B is Boltzmann's constant, T is the temperature in Kelvin, $\Re()$ is the real number operator, and Y is the complex valued transfer

function from a force on the test mass to a velocity of the test mass.

For vertical motion, the force and velocity of Y are both along the vertical degree of freedom. C is about 0.001, which is the coupling from vertical motion to the horizontal longitudinal direction sensed by the interferometer. This value is dominantly due to the curvature of the Earth over the 4 km arms such that the local gravity directions at each end are not parallel. For roll motion, the transfer function Y is along the roll degree of freedom. The coupling factor is assumed to be 3×10^{-6} based on the measurements of the interferometer's response.[10]

To estimate the transfer function Y, state space models for both the BRDs and the suspensions are utilized. The model of the suspension is discussed in detail in Shapiro *et al.*[11] Two BRDs are employed to damp a given mode, one on the left side of the suspension, and one on the right. The BRD model is subtly different depending on this location.

The BRD models, Eqs. (2)–(10), follow the notation of the generalized tuned mass damper in Figure 2, but with a left and right pair of BRDs applied to the suspension as shown in Figure 3. Figure 3 shows the BRDs applied at the UIM springs, for reasons discussed in Section III. This location is equivalent to attaching them to the desired location of the penultimate mass since the suspension wires are effectively rigid in extension at the bounce and roll frequencies. Eqs. (2) and (3) summarize the state space equations for the left and right BRDs, respectively, where $\boldsymbol{x}$ is the displacement and velocity state vector for the BRD damping mass, $\boldsymbol{s}$ is the vertical and roll displacement vector of the suspension penultimate stage, and $\boldsymbol{f}$ is the vertical and roll reaction force and torque vector

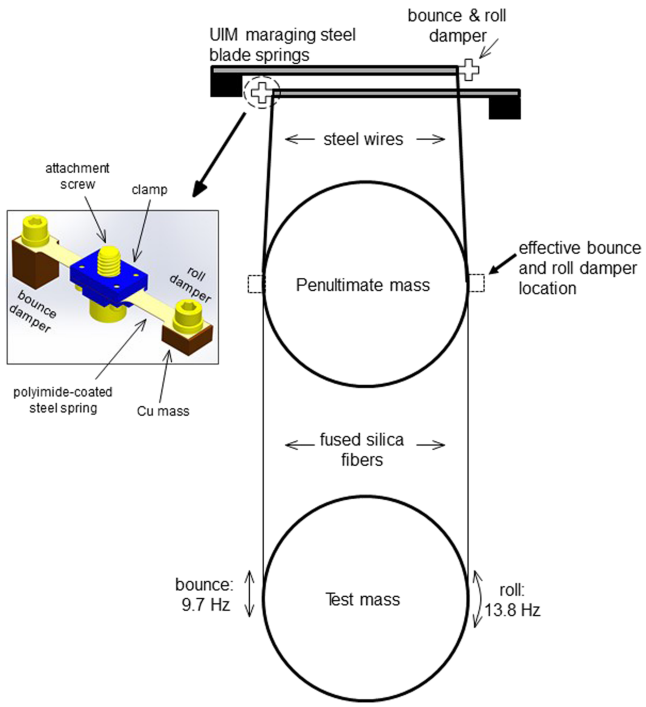

FIG. 3. Diagram showing the final design of the BRDs, indicating where they are attached to the quadruple pendulum. Although the BRDs are on the UIM springs, their effect is projected along the length of the steel wires to the penultimate mass. See also Figure 9 for a close-up view of a BRD attached to the tip of the UIM spring showing its relative orientation.

the BRD applies to the suspension penultimate stage. The subscripts L and R indicate the BRD left or right location on the suspension. $\boldsymbol{A}$, $\boldsymbol{B}$, $\boldsymbol{C}$, and $\boldsymbol{D}$ are the state space matrices as given by Eqs. (4)–(10). The BRD's physical parameters are given by stiffness k, mass m, and mechanical loss factor ϕ (structural damping). n_3 is the horizontal distance from the BRD to the suspension's roll axis. The sign convention is positive for increasing vertical height and roll pointing down the 4 km arm, where left and right are seen from behind the suspension, looking down the arm.

$$\begin{aligned} \boldsymbol{x}_L &= \boldsymbol{A}\dot{\boldsymbol{x}}_L + \boldsymbol{B}_L\boldsymbol{s}, \\ \boldsymbol{f}_L &= \boldsymbol{C}_L\boldsymbol{x}_L + \boldsymbol{D}_L\boldsymbol{s}, \end{aligned} \tag{2}$$

$$\begin{aligned} \boldsymbol{x}_R &= \boldsymbol{A}\dot{\boldsymbol{x}}_R + \boldsymbol{B}_R\boldsymbol{s}, \\ \boldsymbol{f}_R &= \boldsymbol{C}_R\boldsymbol{x}_R + \boldsymbol{D}_R\boldsymbol{s}, \end{aligned} \tag{3}$$

$$\boldsymbol{A} = \begin{bmatrix} 0 & 1 \\ -\frac{k}{m}(1+i\phi) & 0 \end{bmatrix}, \tag{4}$$

$$\boldsymbol{B}_L = \begin{bmatrix} 0 & 0 \\ \frac{k}{m}(1+i\phi) & n_3\frac{k}{m}(1+i\phi) \end{bmatrix}, \tag{5}$$

$$\boldsymbol{B}_R = \begin{bmatrix} 0 & 0 \\ \frac{k}{m}(1+i\phi) & -n_3\frac{k}{m}(1+i\phi) \end{bmatrix}, \tag{6}$$

$$\boldsymbol{C}_L = \begin{bmatrix} k(1+i\phi) & 0 \\ n_3k(1+i\phi) & 0 \end{bmatrix}, \tag{7}$$

$$\boldsymbol{C}_R = \begin{bmatrix} k(1+i\phi) & 0 \\ -n_3k(1+i\phi) & 0 \end{bmatrix}, \tag{8}$$

$$\boldsymbol{D}_L = \begin{bmatrix} -k(1+i\phi) & -n_3k(1+i\phi) \\ -n_3k(1+i\phi) & -n_3^2k(1+i\phi) \end{bmatrix}, \tag{9}$$

$$\boldsymbol{D}_R = \begin{bmatrix} -k(1+i\phi) & n_3k(1+i\phi) \\ n_3k(1+i\phi) & -n_3^2k(1+i\phi) \end{bmatrix}. \tag{10}$$

The BRD models are integrated with the existing suspension models by applying the BRD reaction forces $\boldsymbol{f}$ to the suspension at the penultimate stage, and in turn, applying the penultimate stage displacements $\boldsymbol{s}$ to the BRDs.

The BRD damped suspension model is then used to simulate the thermal noise and bounce and roll Qs for various BRD parameters in order to find a parameter set that meets the requirements.

A convenient parameter for designing the BRD is its mass ratio μ. By definition, this value is given by

$$\mu = 2m/M, \tag{11}$$

where m is the mass of each damper and M is the modal mass of the bounce or roll mode. The factor of 2 reflects the fact that the damping mass is split between the left and right dampers. For bounce, $M = 40$ kg, following the convention of unit length mode shape eigenvectors. For roll, $M = I/{n_3}^2 = 18$ kg, where I is the modal rotational inertia and M is the effective modal mass at distance n_3. This modal domain is convenient because the BRD natural frequency can be tuned as if it was applied to

a single degree of freedom system like that shown in Figure 2, where the mass to be damped is twice the modal mass.

With a tuned mass damper applied, the single degree of freedom system in Figure 2 becomes 2 degrees of freedom with 2 resonant frequencies. For a given mass ratio, the tuned mass damper has an optimal natural frequency ω_0 where the damping of these two resonances is equal. Any detuning results in one of the resonances having less damping. This optimal natural frequency ω_0, in rad/s, which we target for the BRDs, is given by[12]

$$\omega_0 = \frac{1}{1+\mu/2}\Omega = \sqrt{k/m}, \tag{12}$$

where Ω is the frequency of the bounce or roll mode in rad/s.

For a given mass ratio, there is also a loss factor value that yields the smallest possible Q. This optimal loss factor is referred to here as ϕ^*. Figure 4 shows the optimal loss in blue and the 20 Hz thermal noise in red as a function of the mass ratio μ. Figure 5 shows the Qs achieved with the optimal loss ϕ^* and with 0.1% and 1% detuning of the BRD natural frequency as a function of mass ratio μ. Generally, larger mass ratios permit more damping and a greater tolerance for BRD natural frequency detuning at the expense of more thermal noise.

We note that the thermal noise curve shown in Figure 4 assumes that the BRD loss is structural in nature (ϕ constant with frequency). We have also carried out modeling assuming viscous damping (ϕ proportional to frequency). This raises the thermal noise level slightly by 20 Hz, but it is not significantly different.

B. Target damped Q and implications for BRD parameters from modelling

As noted in the Introduction, the current undamped Qs for the bounce and roll modes of the quadruple suspension are on average 5×10^5 under vacuum. Typically the modes can get excited to levels 3–4 orders of magnitude above the thermal excitation level when rung up. We would like the BRDs to reduce the modes to their thermal levels in ~100 s. Noting that with a lower Q, the modes will not build up as much in the first place by the ratio of the damped Q, Q_d, to the original Q,

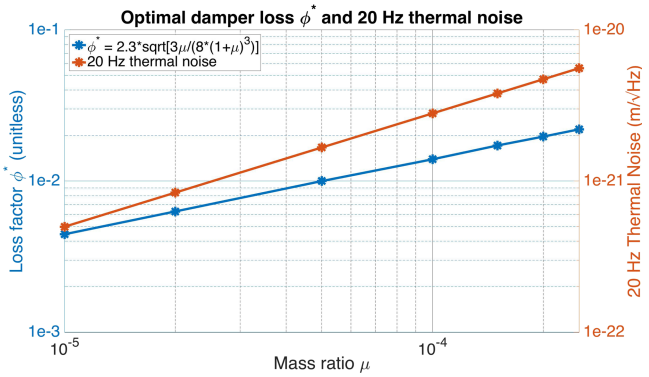

FIG. 4. Blue: the optimal loss factor ϕ^* that yields the smallest bounce and roll Qs, where the damper stiffness is given by $k(1+i\phi)$. This loss is also known as structural damping. Red: the sum of the vertical and roll 20 Hz thermal noise with the optimal loss ϕ^*.

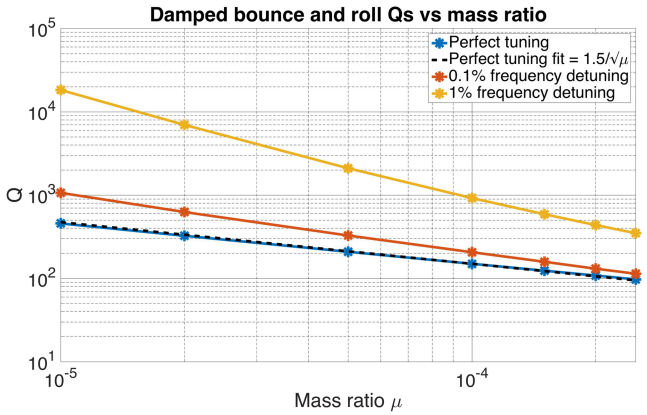

FIG. 5. The smallest possible Qs of the bounce and roll modes. The blue line is the Q achieved with a perfectly tuned damper. The red and yellow lines show the Qs for dampers detuned by 0.1% and 1%, respectively, in frequency. The dotted black line is a fit to the perfectly tuned case.

the time τ to decay to 1/e given an original excitation of 10^4 above thermal level should satisfy[13]

$$\log_e\left(10^4 \frac{Q_d}{500\,000}\right)\tau < 100\,\mathrm{s}. \tag{13}$$

We also note that $Q_d = \pi\tau f \approx 10\pi\tau$, where f is the bounce or roll mode frequency. Hence

$$\log_e\left(\frac{Q_d}{50}\right) Q_d < \pi \times 10^3. \tag{14}$$

This is satisfied for $Q_d < 1000$. With an excitation level of 10^3, the corresponding condition is $Q_d < 2000$. We thus targeted a Q_d value in our design of one to several thousands.

We took as a working target that the additional thermal noise due to the addition of the BRDs should be less than the intrinsic thermal noise at 20 Hz, which is $\sim 1.6 \times 10^{-20}$ m/√Hz.[5] From Figure 4, a mass ratio of $\mu = 5 \times 10^{-5}$, corresponding to dampers with bounce mass ~1 g and roll mass ~0.5 g, achieves an order of magnitude less noise than this. In addition such a mass ratio yields a Q for the bounce and roll modes of 2000 assuming that the optimal damping factor for the BRD is used and for a 1% detuning as shown in Figure 5, which we regarded as a reasonable tuning value to meet. Thus our initial design of damper used those mass values.

III. DESIGN

The conceptual design for the BRDs is discussed in Fritschel[13] and the final version of the design is shown in Figure 3, which also indicates where the BRDs are attached to the quadruple suspension. The basic idea is to attach a mass to the end of a cantilever spring blade, with the mass chosen to satisfy the thermal noise requirements as in Section II above, and the cantilever parameters then chosen to give the desired frequency. By making the cantilever double ended with different masses, one damper unit can be used to damp both bounce and roll modes. For symmetry two units are used, one attached to the tip of each maraging steel blade at the upper intermediate mass of the quad directly supporting the penultimate mass. We note that it would be desirable if the BRDs could be directly attached to the penultimate mass itself, but

since there was not a simple way to do this, given that those masses are made from fused silica, we chose the maraging steel spring tips at the stage above, which are essentially directly coupled to the penultimate mass at the frequencies of interest. For the first tests, copper was chosen as the cantilever and mass material since it has a relatively high loss factor for a metal, and eddy current damping was envisioned as an add-on, to be used if the copper itself proved not to give enough damping. The masses were initially joined to the cantilever blade by soldering.

IV. RESULTS FROM INITIAL LAB TESTS AND DEVELOPMENT OF FINAL DESIGN

A. Initial work using copper sheet for the BRD blades

The first BRD was assembled using 0.002 in. (51 μm) Cu sheet for the blade. Initial testing was done of the damper on its own. Several issues were observed. First the blade ends sagged appreciably with the weight of the Cu masses. Second the modal frequencies of the damper changed with time, which was attributed to the sag changing over time. Third the amount of damping was not significant. We noted that using the eddy current damping as first envisioned would be challenging to align due to the sag and so investigated the application of several types of lossy material to the top surface of the blade to add damping.

For our next set of prototypes, we changed to hardened Cu material to reduce sag. We attached the masses using screws since we realized that the soldering temperature was close to the annealing temperature of Cu so that we were likely affecting the BRD's properties by soldering. Having investigated various possible lossy materials, we chose to use Pyralux,[14] type LF0110, a polyimide film typically used for making flexi-circuits, coated on one side with acrylic adhesive which forms a strong bond when assembled using raised temperature and pressure. We used 25 μm thick Pyralux with 25 μm adhesive layer. The masses used were ~1.7 g (for bounce) and ~0.8 g (for roll). These were slightly heavier than those used in the first BRD since the Pyralux slightly stiffens the blades as well as adding damping.

Initial tests of this BRD design on its own were more promising. To test the BRDs as tuned dampers, we built an all-metal mock-up of the two lowest stages of a quadruple pendulum, suspended from a set of maraging steel blades to which the BRDs were attached. See Figure 6. The attachment made use of an existing fastener at the tip of the maraging steel blade which was used to hold the clamp by which the suspension wires were attached. This double pendulum was placed in a vacuum tank so that the system could be tested under vacuum. The thickness of the wires suspending the lowest mass was chosen to give frequencies close to those for the full quadruple pendulum with silica fibers. To sense and excite the relevant modes, we set up a BOSEM[15] (Birmingham design of optical sensor and electromagnetic actuator) pushing vertically on the bottom mass, situated off-axis so that vertical or roll motion could be excited, as indicated in Figure 6. We recorded the data from the sensor using a data logger and analysed the results using the curve fitting application in MATLAB.[16]

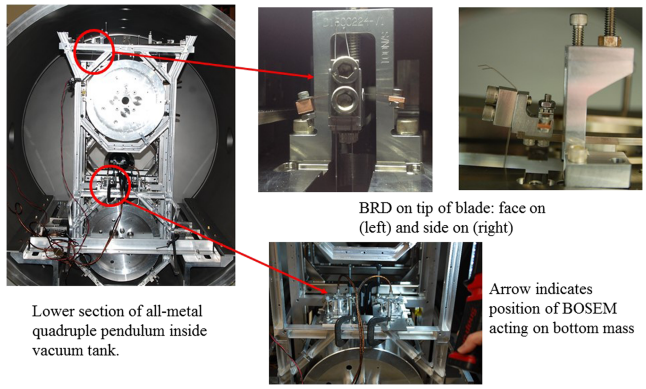

FIG. 6. Pictures of the setup used at Caltech for testing the BRDs under vacuum. The acronym BOSEM is defined in Section IV of the text.

To achieve matching of the damper frequencies to those of the relevant modes to ~1%, we had to retune the BRDs in the vacuum tank. We found that the precise way we assembled and clamped the BRDs onto the maraging steel blade spring tips altered the frequency by more than our acceptable tuning range. The method by which we achieved the desired BRD frequencies was to manually alter the angle of the copper blades, which was clearly not ideal. However we did see damping of the highest bounce and roll modes of our double pendulum, reducing the undamped Qs of around 2800 for bounce and 1600 for roll to damped values averaging around 730 and 630, respectively. We also noted that the damping changed with time which we attributed to the tuning changing as sag of the BRDs changed.

B. Final design and testing using steel for the BRD blades

To address the issues of changing frequency over time, we considered a design using stiffer 0.003 in. (75 μm) Cu sheet for the blade, which meant that the masses had to be increased accordingly. We monitored the behavior of this design of BRD, attaching the unit rigidly to the floor, and measuring its frequency using a laser vibrometer sensor connected to a Bruel and Kjaer modal analysis system.[17] We still observed the frequency increasing slowly monotonically over a week, so we decided to try 0.002 in. steel, which proved to be much more stable, with essentially no drift. We also incorporated a sandwich clamp design permanently attached to the BRD, as seen in Figure 3, to aid in handling and to reduce frequency changes during installation procedures. The masses used with this design were ~3.3 g and ~1.5 g for the bounce and roll mode ends, respectively. To tune the frequencies, we obtained a library of Cu masses, differing by ~0.1 g. Using these in combination with washers of various sizes, we could obtain the desired frequencies, noting that the tolerances on the as-received blades were such that each BRD had to be individually tuned. The Qs of this design of damper, attached to the floor, using 2 thou steel, measured in air, were 190 for the bounce and 175 for the roll.

With this BRD design applied to the double pendulum, we achieved significant damping. We monitored the Q values over several weeks under vacuum and achieved an average value for

the bounce mode of around 860 and for the roll mode around 470 where, as noted above, the undamped Qs were ~2800 for bounce and ~1600 for roll. See Figures 7 and 8 for examples of the decays obtained for bounce and roll, respectively. We did see some variability typically of order ±100 on the Q values. We noticed that the measured Q depended on where in the decay curve the fit was carried out, suggesting that the frequency of the BRD and hence the tuning was varying slightly with amplitude of excitation. We could also see beats in some of the decay curves, in particular for the bounce mode, visible in Figure 7. This is not surprising, since in fact we are exciting a three-coupled system consisting of the main pendulum and the two BRDs, all with slightly different frequencies and quality factors. The beat period typically lay between ~10 and ~20 s which for a nominal resonant frequency of 10 Hz corresponds to a frequency difference between 0.05 and 0.1 Hz or detuning of 0.5% to 1%. We used the model discussed in Section II to test whether the results we obtained tied up with the theory. The model predicted Qs typically slightly higher than observed but in the same range allowing for errors.

We noted that putting these same dampers on the monolithic quadruple suspensions where the undamped Qs are much higher, we would expect from our model that the damped Qs would lie in the desired range of one to a few thousand assuming similar tuning.

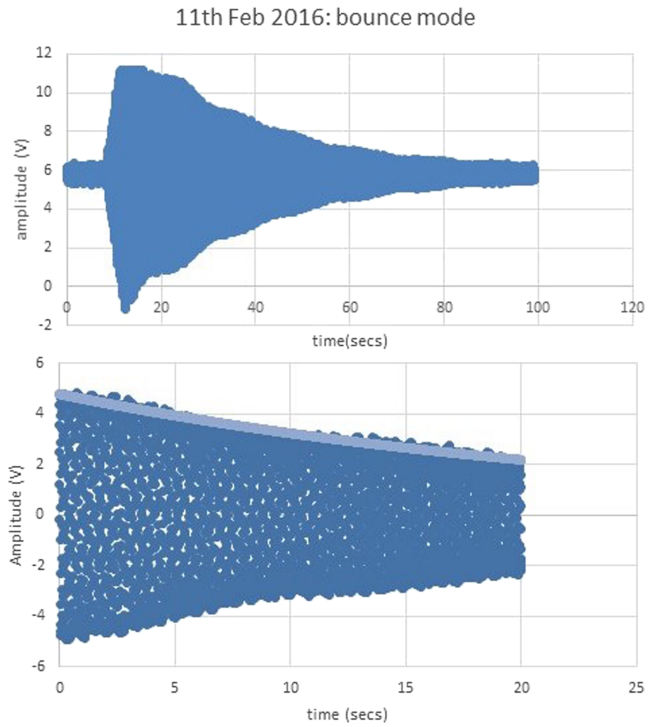

FIG. 7. Example of decay curve for the bounce mode of the lower stage of the double pendulum at Caltech. The y axis gives the amplitude of the BOSEM signal in volts which is proportional to the vertical displacement of the test mass. The top trace shows the full data set. The lower trace shows a shorter section of the data (22–42 s), with the mean value of BOSEM signal subtracted to show the motion about the mean. A fitted amplitude is overlaid on the data, obtained using a MATLAB curve fitting routine for an exponentially decaying sinusoid. The fit gave a frequency f = 9.9 Hz and Q = 795 with a goodness of fit value for R^2 of 0.996. The beat signal discussed in the text can clearly be seen in the top trace.

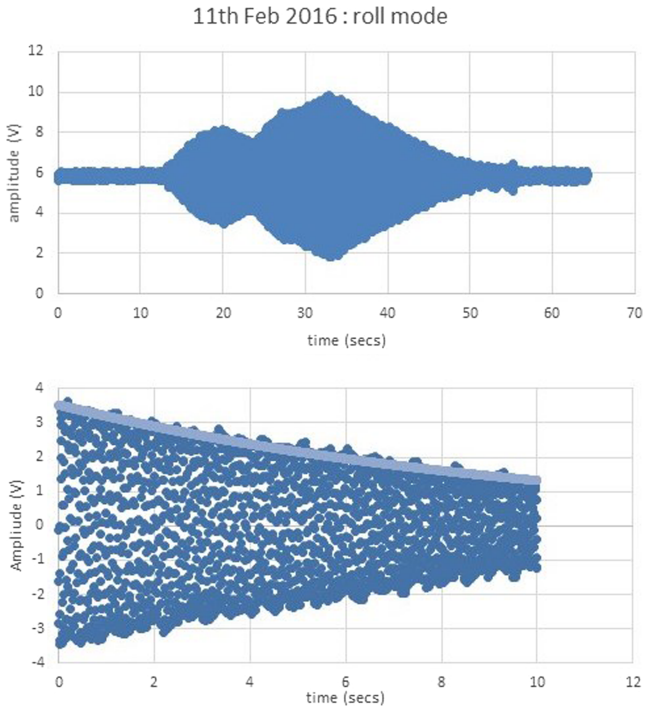

FIG. 8. Example of decay curve for the roll mode of the lower stage of the double pendulum at Caltech. The y axis gives the amplitude of the BOSEM signal in volts which is proportional to the angular displacement in roll of the test mass. The top trace shows the full data set. The lower trace shows a shorter section of the data (35–45 s), with the mean value of BOSEM signal subtracted to show the motion about the mean. A fitted amplitude is overlaid on the data, obtained using a MATLAB curve fitting routine for an exponentially decaying sinusoid. The fit gave a frequency f = 13.7 Hz and Q = 440 with a goodness of fit value for R^2 of 0.992.

Given these encouraging results, we proceeded to produce further BRDs using the same design for installation at the observatories. One final change we made was to the method of attachment for the BRDs to the existing suspensions. Our first method, which made use of the existing fastener holding the wire clamps to the maraging steel blade tip, would require significant disassembly of the upper intermediate mass of the quadruple pendulum to gain access. An alternative method, using a "piggyback" clamp which fits over the end of the quad blade and requires no disassembly of existing parts, was found

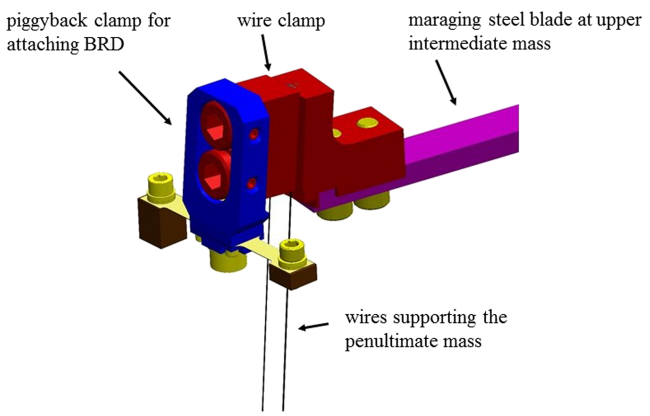

FIG. 9. Drawing showing the use of a piggyback clamp for attaching the BRD to the existing wire clamp on the end of the maraging steel blade.

to work well in tests and was chosen as the preferred method of attachment. See Figure 9.

V. FINAL RESULTS AND CONCLUSIONS

To date, BRDs have been installed on the four test mass suspensions at the LIGO Livingston Observatory (LLO). Average masses for the bounce and roll ends were ~3.3 and 1.7 g, respectively, corresponding to mass ratios of $\sim 1.65 \times 10^{-4}$ and 1.9×10^{-4}, respectively. The quality factors for the BRDs alone were around 170 and 190, respectively, corresponding to loss values 5.9×10^{-3} and 5.3×10^{-3}, which are slightly less damping than the optimum shown in Figure 4 for the corresponding mass ratios. With these parameters, we estimate the thermal noise contribution from the BRDs as a function of detuning to be as shown in Figure 10. Also shown in this figure are the expected Q values for bounce and roll with these parameters, for various detuning values. We note that the thermal noise level at 20 Hz from the BRDs is at most $\sim 2.6 \times 10^{-21}$ m/$\sqrt{\text{Hz}}$ which satisfies our target of lying significantly below the intrinsic thermal noise level. If we model the damping as viscous in nature, the additional thermal noise at 20 Hz would be slightly higher, $\sim 2.8 \times 10^{-21}$ m/$\sqrt{\text{Hz}}$, but still acceptable.

The Qs of the bounce and roll modes for all of the suspensions under vacuum have been investigated by exciting the modes and then turning off the excitation and observing the ringdown.[18] For the bounce modes, the Qs range from 4500 to 9000. For the roll modes, two have been observed with Qs of 1700 and 2600. The other two could not be rung up, suggesting that their Q values are lower than the observed roll modes. If we compare the observed Qs with the expected values for various detuning levels as given in Figure 10, we conclude it likely that the tuning of the bounce ends of the BRDs has moved from our target of ~1% to values in excess of 3% for the ones around 9000. The roll detuning is smaller, somewhere between 1% and 2% for those we have observed, and likely better than 1% for the two which remain unobserved. The decay times range from ~40 s for the lowest observed roll Qs to ~300 s for the highest observed bounce Qs.

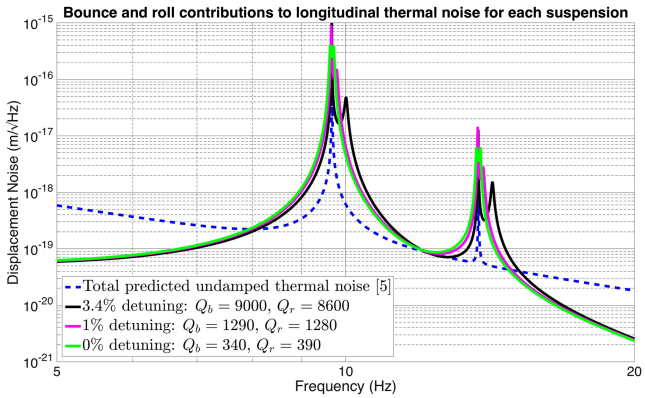

FIG. 10. Modeled graphs of bounce and roll contributions to longitudinal thermal noise for the parameters of the design of BRDs installed at the LIGO Livingston Observatory. The Q values for various detuning values are also shown, where b = bounce, r = roll. For reference, the dashed curve is a prediction of the total intrinsic thermal noise in the longitudinal direction for the suspension prior to the addition of bounce and roll dampers (based on Ref. 6).

When we prepared the BRDs at Caltech, we aimed for an average of around ~1% or less detuning. We did not check the tuning after sending the BRDs to LLO. We have since found that very small adjustments in positioning and tightening of the masses on the blades, such as could result from handling while in transit, can significantly affect the tuning. Our procedure for future installations will call for re-measurement and retuning as needed just prior to installation. In addition if we were to procure parts for more BRDs, we would consider tightening the tolerances, particularly on the holes in the steel blades to which the masses are attached, since we have found we can significantly change the frequencies by loosening and retightening the masses in a slightly different position.

Despite the Qs for the bounce modes being more than we originally targeted, the use of the BRDs has made a very significant positive impact on the running of the interferometer. Active damping of the bounce and roll modes is no longer required, and the use of the BRDs has also relaxed constraints on various length and angular control loops. The time taken while waiting for the modes to damp down has reduced from hours to a few minutes or less, effectively removing one major source of loss of observing time at LLO. We look forward to completing this work by installing BRDs at the LIGO Hanford Observatory in due course.

ACKNOWLEDGMENTS

We wish to thank colleagues in the LIGO Scientific Collaboration for their support and interest in this work. We thank our colleagues at the LIGO Livingston Observatory for taking data on the BRD performance *in situ*. We also acknowledge the following colleagues for input on various aspects of the design and implementation of the BRDs: Ben Abbott, Rich Abbott, Stuart Aston, Dennis Coyne, Brian Lantz, Travis Sadecki, Eddie Sanchez, Evan Sloan, Bob Taylor, Gary Traylor, and Betsy Weaver. We acknowledge the support provided by the National Science Foundation for this work. LIGO was constructed by the California Institute of Technology and Massachusetts Institute of Technology with funding from the National Science Foundation and operates under Cooperative Agreement No. PHY-0757058. Advanced LIGO was built under Award No. PHY-0823459. The work at Stanford University is supported by Cooperative Agreement No. PHY-1404430. This paper has LIGO document No. P1600328.

[1] B. P. Abbott *et al.* (LIGO Scientific Collaboration and Virgo Collaboration), "Observation of gravitational waves from a binary black hole merger," Phys. Rev. Lett. **116**, 061102 (2016).
[2] B. P. Abbott *et al.* (LIGO Scientific Collaboration and Virgo Collaboration), "GW151226: Observation of gravitational waves from a 22-solar-mass binary black hole coalescence," Phys. Rev. Lett. **116**, 241103 (2016).
[3] J. Aasi *et al.* (LIGO Scientific Collaboration), "Advanced LIGO," Class. Quantum Grav. **32**, 074001 (2015).
[4] B. P. Abbott *et al.* (LIGO Scientific Collaboration and Virgo Collaboration), "GW150914: The advanced LIGO detectors in the era of first discoveries," Phys. Rev. Lett. **116**, 131103 (2016).
[5] S. M. Aston *et al.*, "Update on quadruple suspension design for advanced LIGO," Classical Quantum Gravity **29**, 235004 (2012).
[6] A. V. Cumming *et al.*, "Design and development of the advanced LIGO monolithic fused silica suspension," Classical Quantum Gravity **29**, 035003 (2011).

[7]S. M. Aston, "Optical read-out techniques for the control of test-masses in gravitational wave observatories," Ph.D. thesis, The University of Birmingham, 2011, available at https://dcc.ligo.org/LIGO-P1300051/public.
[8]B. Shapiro, "Tuned mass damper simulations for quad bounce and roll modes," LIGO document number T1500271-v7, https://dcc.ligo.org/LIGO-T1500271/public (2015).
[9]P. Saulson, *Fundamentals of Interferometric Gravitational Wave Detectors* (World Scientific, 1994).
[10]See https://alog.ligo-wa.caltech.edu/aLOG/index.php?callRep=19649 for information on coupling factor for roll motion.
[11]B. Shapiro, M. Barton, N. Mavalvala, R. Mittleman, and K. Youcef-Toumi, "Selection of important parameters using uncertainty and sensitivity analysis," IEEE/ASME Trans. Mechatronics **20**(1), 13 (2015).
[12]J. P. Den Hartog, *Mechanical Vibrations*, 3rd ed. (McGraw-Hill, 1947).
[13]P. Fritschel, "Concept for a bounce & roll mode damper for the quad suspensions," LIGO document T1500343-v1, https://dcc.ligo.org/LIGO-T1500343/public (2015).
[14]See http://www.dupont.com for information on Pyralux.
[15]L. Carbone *et al.*, "Sensors and actuators for the advanced LIGO mirror suspensions," Classical Quantum Gravity **29**, 115005 (2012).
[16]See https://www.mathworks.com/products/matlab/ for information on MATLAB.
[17]See https://www.bksv.com/en/products/PULSE-analysis-software for information on the Bruel and Kjaer pulse analysis software.
[18]See https://alog.ligo-la.caltech.edu/aLOG/index.php?callRep=28503 for information on measured Q values at LIGO Livingston Observatory.